

Low-lying level structure of Λ hypernuclei and spin dependence of ΛN interaction with antisymmetrized molecular dynamics

Masahiro Isaka¹, Yasuo Yamamoto², and Toshio Motoba^{3,4}

¹ *Science Research Center, Hosei University, 2-17-1 Fujimi, Chiyoda, Tokyo 102-8160, Japan*

² *RIKEN Nishina Center, Wako, Saitama 351-0198, Japan*

³ *Laboratory of Physics, Osaka Electro-Communication University, Neyagawa 572-8530, Japan and*

⁴ *Yukawa Institute for Theoretical Physics, Kyoto University, Kyoto 606-8502, Japan*

(Dated: December 16, 2021)

ΛN spin-spin and spin-orbit splittings in low-lying excitation spectra are investigated for p -shell Λ hypernuclei on the basis of the microscopic structure calculation within the antisymmetrized molecular dynamics, where the ΛN G -matrix interaction derived from the baryon-baryon interaction model ESC (extended soft core) is used. It is found that the ground-state spin-parity is systematically reproduced in the p -shell Λ hypernuclei by tuning the ΛN spin-spin and spin-orbit interactions so as to reproduce the experimental data of ${}^4_\Lambda\text{H}$, ${}^7_\Lambda\text{Li}$ and ${}^9_\Lambda\text{Be}$. Furthermore, we also focus on the excitation energies of the excited doublets as well as the energy shifts of them by the addition of a Λ particle.

PACS numbers: Valid PACS appear here

I. INTRODUCTION

Hypernuclear physics makes substantial progress by both theoretical and experimental works in the last decades. In particular, experimental information of Λ hypernuclei has been increased by the counter experiments such as (π^+, K^+) reactions [1]. Combined with the γ -ray spectroscopy techniques, the low-lying level structure of Λ hypernuclei have been revealed precisely. Recently, the $(e, e'K^+)$ reaction experiments have been developed at Thomas Jefferson Laboratory (JLab), where the absolute values of binding energies are expected to be measured in a wide mass region including medium-heavy hypernuclei with high resolution. These data of hypernuclei are essential to understand hyperon-nucleon (YN) interactions, because YN scattering experiments are rather difficult due to short life-time of hyperons. For example, from the analysis of the binding energies of Λ hypernuclei, B_Λ , one can evaluate the depth of the single-particle potential of a Λ particle, U_Λ , in nuclear matter. In associated with the developments on baryon-baryon interaction models [2–8], an important role of the $\Lambda N - \Sigma N$ coupling to give a reasonable U_Λ value in nuclear matter has been revealed.

Based on the precise data of Λ hypernuclei, structure of hypernuclei is also investigated and becomes one of the important issues. Especially, structure of light Λ hypernuclei is of interest because ordinary nuclei in p -shell and sd -shell mass regions have various structures such as cluster and deformed mean-field like structures near the ground states. For example, in ${}^7_\Lambda\text{Li}$ [9–12], it was predicted that the addition of a Λ particle reduces the intercluster distance between α and d of the core nucleus ${}^6\text{Li}$, which was confirmed through the observations of the $B(E2)$ values by the γ -ray spectroscopy experiment. In the other Λ hypernuclei such as ${}^{13}_\Lambda\text{C}$, several theoretical calculations showed that a Λ particle reduces the nuclear quadrupole deformation of the ground states [13–20].

In addition, the coexistence of pronounced cluster and mean-field like structures in core nuclei can cause changes of level ordering in excitation spectra, which were predicted in p - and sd -shell Λ hypernuclei such as ${}^{13}_\Lambda\text{C}$ [21] and ${}^{21}_\Lambda\text{Ne}$ [22]. Furthermore, it was pointed out that size differences between the ground and excited states in p -shell nuclei lead to energy shifts of excited states in the corresponding hypernuclei [23].

The structure of core nuclei also affects the systematics of B_Λ values through the density dependence of the Λ -nucleon (ΛN) interaction, which was investigated by the authors (M. I. and Y.Y.) with structure calculations within the framework of the antisymmetrized molecular dynamics for hypernuclei (HyperAMD) adopting the G -matrix interactions (called YNG) as a ΛN effective interaction [24, 25]. The YNG interactions are obtained by the G -matrix calculation in nuclear matter from the Nijmegen Extended Soft-Core (ESC) potentials, which depend on the nuclear Fermi momentum k_F . In Refs. [24, 25], the authors succeeded in reproducing the existing B_Λ data as a function of mass number A , namely the mass dependence of B_Λ , where the averaged density approximation (ADA) is applied to treat the k_F dependence. This is achieved by the developments of the interaction models and microscopic calculation of hypernuclear structure. In Ref. [25], it was also found that fine tuning of the ΛN YNG interactions is still necessary to describe the level ordering of the ground-state spin doublet partners properly, which is one of the purposes of the present paper.

The level ordering of the spin doublets is mainly determined by properties of spin-dependent parts of ΛN interactions, namely the ΛN spin-spin and spin-orbit interactions, because the spin doublet states in Λ hypernuclei are generated by the coupling between the non-zero spin of the core states and the Λ particle with spin 1/2. For the spin-spin part, the historically important data were the spin doublet $(0^+, 1^+)$ states of ${}^4_\Lambda\text{He}$ (${}^4_\Lambda\text{H}$). These

hypernuclear data were first used for the parameter fitting of the hyperon-nucleon one-boson exchange model NSC97 [3]. Among 6 versions (a,b,c,d,e,f) with different spin-spin interactions, NSC97f was found to reproduce reasonably the above data of spin doublet splitting. Furthermore, the spin doublet states of ${}^{12}_{\Lambda}\text{C}$ and ${}^{11}_{\Lambda}\text{B}$ were shown to be described well by the shell-model analysis with the G -matrix interaction derived from NSC97f [26]. On the other hand, spin-orbit splittings also were long-standing problems in hypernuclear physics. Qualitatively, small values of splitting energies are obtained by large cancellations between symmetric LS (SLS) and anti-symmetric LS (ALS) contributions. In the case of using the G -matrix interaction from NSC97f, however, the cancellation was shown to be not enough to reproduce quantitatively the small value of the experimental data [27, 28].

The ESC model [5] was proposed in order to improve important deficiencies of NSC97, where two-meson and meson-pair exchanges were taken into account explicitly instead of “effective bosons” in one-boson-exchange models such as NSC97. In the ESC models, then, the spin-spin parts in even states were designed to give similarly those of NSC97f, and the SLS and ALS parts were done to cancel more substantially than those of NSC97f. The shell-model analysis for spin doublet splittings in ${}^{12}_{\Lambda}\text{C}$ and ${}^{11}_{\Lambda}\text{B}$ were performed by using the G -matrix interactions derived from the ESC models [26]. The obtained values of splitting energies were rather larger than those for NSC97f, namely than the experimental values, because the odd-state interactions in the former were rather different from those in the latter. These results are consistent with the incorrect ordering of the doublet partners in Refs. [25].

The aim of this paper is to study spin-spin and spin-orbit splittings in excitation spectra of Λ hypernuclei systematically. For the present purpose we will especially investigate necessary corrections in both even- and odd-state spin-dependent parts of the YNG interactions so as to reproduce the excitation spectra of p -shell Λ hypernuclei. Thus, we will finally propose a revised version of the YNG interactions which can be applicable to whole mass regions of hypernuclei.

This paper is organized as follows. In the next Section, the theoretical framework of HyperAMD is explained. In Sec. III, we discuss the spin-doublet splittings obtained in a schematic model in order to suggest leading properties in spherical hypernuclei. In Sec. IV, we discuss the effects of the ΛN spin-spin and spin-orbit interactions by showing the excitation spectra of the hypernuclei as well as those of the core nuclei. Section V summarizes this work.

II. THEORETICAL FRAMEWORK

In this paper, we apply an extended version of the antisymmetrized molecular dynamics for hypernuclei named

HyperAMD to several p -shell Λ hypernuclei basically following Refs. [24, 25]. This model enables us to describe various nuclear structures and to investigate the dynamical changes caused by the addition of a Λ particle in the hypernuclei around the p - sd shell regions.

A. Hamiltonian

The Hamiltonian used in this study is given as

$$H = T_N + T_{\Lambda} - T_g + V_{NN} + V_C + V_{\Lambda N}, \quad (1)$$

where T_N , T_{Λ} , and T_g are the kinetic energies of the nucleons, Λ particle, and center-of-mass motion, respectively. V_{NN} is the effective nuclear force. The Coulomb interaction V_C is approximated by the sum of seven Gaussians.

We use the Gogny D1S force [29, 30] as the effective nuclear force V_{NN} . One of the characteristics of Gogny D1S is the density-dependent interaction acting as a repulsive force at high density, which is essential to describe nuclear saturation property. As discussed in Refs. [24, 25], for reproducing the B_{Λ} values systematically, it is indispensable to describe structure of core nuclei, especially core deformation, properly. The Gogny D1S force is one of the effective interactions that gives better description of nuclear deformation and reasonable values of the nuclear binding energies for the ground states of normal nuclei in a wide mass region. In this study, since we focus on the effects by the spin-dependent part of the ΛN interaction, it is necessary to describe excitation spectra of the core nuclei properly as well as possible. Though the Gogny D1S describes structure of the ground states, it may give small deviation of energies for excited states from the observed data. In such cases, for the quantitative discussion, we slightly change the parameter sets of the Gogny D1S or use the Volkov No. 2 force [31] instead, which is discussed in Sec. IV A in detail.

B. ΛN interaction

As for the ΛN effective interaction $V_{\Lambda N}$, we use the G -matrix interaction derived from the Nijmegen ESC potential, ESC14, where the ΛN - ΣN coupling is renormalized by the G -matrix calculation. As shown in Ref. [25], using the ESC14 force with the many-body effects (ESC14+MBE), the HyperAMD calculation nicely reproduces the existing data of B_{Λ} systematically. However, level ordering of spin doublet partners is incorrect in several p -shell Λ hypernuclei. In this paper, we investigate spin-spin and spin-orbit splittings of the p -shell Λ hypernuclei using ESC14+MBE, where the k_F dependence of the G -matrix interaction is treated by the ADA procedure in the same way as in Refs. [24, 25]. Furthermore, we also apply the NSC97f for the comparison. In the case of NSC97f, its strong odd-state repulsions play an

important role to reproduce the mass dependence of B_Λ instead of the above MBE.

The ΛN G -matrix interaction $V_{\Lambda N}$ is composed of the central ($V_{\Lambda N}^{\text{cent}}$) and spin-orbit ($V_{\Lambda N}^{\text{LS}}$) forces, namely $V_{\Lambda N} = V_{\Lambda N}^{\text{cent}} + V_{\Lambda N}^{\text{LS}}$. The ΛN central force $V_{\Lambda N}^{\text{cent}}$ is written as,

$$V_{\Lambda N}^{\text{cent}} = v(^{1E})\hat{P}(^1E) + v(^{3E})\hat{P}(^3E) + v(^{1O})\hat{P}(^1O) + v(^{3O})\hat{P}(^3O), \quad (2)$$

where

$$v^{(c)}(k_F, r) = \sum_{i=1}^3 (a_i^{(c)} + b_i^{(c)}k_F + c_i^{(c)}k_F^2)e^{-r^2/\beta_i^2}, \quad (3)$$

$$c = ^1E, ^3E, ^1O \text{ or } ^3O. \quad (4)$$

The parameters $a_i^{(c)}$, $b_i^{(c)}$ and $c_i^{(c)}$ of ESC14+MBE are shown in Tab. I for all channels, which are the same as used in Ref. [25]. Using the Pauli's spin matrix $\vec{\sigma}$, one can rewrite $V_{\Lambda N}^{\text{cent}}$ as

$$V_{\Lambda N}^{\text{cent}} = \sum_{i=1}^3 \{ (v_0^{E(i)} + v_\sigma^{E(i)}\vec{\sigma} \cdot \vec{\sigma})\hat{P}(E) + (v_0^{O(i)} + v_\sigma^{O(i)}\vec{\sigma} \cdot \vec{\sigma})\hat{P}(O) \} e^{-r^2/\beta_i^2}, \quad (5)$$

where $\hat{P}(E)$ and $\hat{P}(O)$ are the projectors for the even and odd parity states, respectively. Thus, the spin-spin even and odd parity interactions act through the ΛN central force.

The ΛN spin-orbit force $V_{\Lambda N}^{\text{LS}}$ consists of the symmetric and asymmetric LS (SLS and ALS) components. Each of SLS and ALS of ESC14+MBE is also given by the same functional form as Eq.(3) with $c = \text{SLS}$ or ALS , where the parameters $a_i^{(c)}$, $b_i^{(c)}$, $c_i^{(c)}$ and β_i are listed in Tab. II.

In our G -matrix interaction, the ΛN - ΣN coupling interactions of ESC14 are renormalized into the effective central interactions. It is possible, then, to obtain residual ΛN - ΛN and ΛN - ΣN interactions composed of central and tensor parts, though they are not used in this work. In Ref.[26] such residual interactions were obtained for some versions of the ESC model, to which those for ESC14 are more or less similar.

C. Wave Function

The variational wave function of a single Λ hypernucleus is described by the parity-projected wave function, $\Psi^\pm = P^\pm A\{\varphi_1, \dots, \varphi_A\} \otimes \varphi_\Lambda$, where

$$\varphi_i \propto e^{-\sum_\sigma \nu_\sigma (r_\sigma - \bar{Z}_{i\sigma})^2} \otimes (u_i\chi_\uparrow + v_i\chi_\downarrow) \otimes (\text{p or n}), \quad (6)$$

$$\varphi_\Lambda \propto \sum_{m=1}^M c_m e^{-\sum_\sigma \nu_\sigma (r_\sigma - \bar{z}_{m\sigma})^2} \otimes (a_m\chi_\uparrow + b_m\chi_\downarrow). \quad (7)$$

The single-particle wave packet of a nucleon φ_i is described by a single Gaussian, whereas that of Λ , φ_Λ , is

TABLE I: Parameters of the ΛN central force of ESC14+MBE represented by the three range Gaussian forms given in Eq. (3). $a_i^{(c)}$ [MeV], $b_i^{(c)}$ [MeV · fm], $c_i^{(c)}$ [MeV · fm²] and β [fm] are given for each i . Parameters after the tuning done in Sec. IV B are also shown in parenthesis.

	i	1	2	3
c	β_i	0.50	0.90	2.00
1E	$a_i^{(^1E)}$	-3434.0	416.71(413.11)	-1.708
	$b_i^{(^1E)}$	6937.0	-1108.74	0.0
	$c_i^{(^1E)}$	-2635.0	444.74	0.0
3E	$a_i^{(^3E)}$	-1933.0	214.56(215.76)	-1.295
	$b_i^{(^3E)}$	4698.0	-782.11	0.0
	$c_i^{(^3E)}$	-1974.0	357.4	0.0
1O	$a_i^{(^1O)}$	206.1	94.2(4.2)	-0.8292
	$b_i^{(^1O)}$	-30.52	-39.47	0.0
	$c_i^{(^1O)}$	16.23	66.481	0.0
3O	$a_i^{(^3O)}$	2327.0	-229.15(-199.15)	-0.9959
	$b_i^{(^3O)}$	-2361.0	130.68	0.0
	$c_i^{(^3O)}$	854.3	23.02	0.0

represented by a superposition of Gaussian wave packets. The variational parameters \bar{Z}_i , \bar{z}_m , ν_σ , u_i , v_i , a_m , b_m , and c_m are determined to minimize the total energy under the constraint on the nuclear quadrupole deformation (β, γ), and the optimized wave function $\Psi^\pm(\beta, \gamma)$ is obtained for each given (β, γ).

After the energy variation, we project out the eigenstate of the total angular momentum J for each set of (β, γ),

$$\Psi_{MK}^{J\pm}(\beta, \gamma) = \frac{2J+1}{(8\pi)^2} \int d\Omega D_{MK}^{J*}(\Omega) R(\Omega) \Psi^\pm(\beta, \gamma). \quad (8)$$

The numerical integration is performed for the three Euler angles Ω . To obtain both the ground and excited states of hypernuclei, we also perform the generator coordinate method (GCM) calculation, namely superposition of the different K and (β, γ) values as

$$\Psi_n^{J\pm} = \sum_p \sum_{K=-J}^J c_{npK} \Psi_{MK}^{J\pm}(\beta_p, \gamma_p), \quad (9)$$

where n represents quantum numbers other than total angular momentum and parity. The coefficients c_{npK} are determined by solving the Griffin-Hill-Wheeler equation.

III. DOUBLET ENERGY SPLITTING IN A SCHEMATIC MODEL

Before going to discuss results of the detailed Hyper-AMD calculations, we point out some schematic relations

TABLE II: Same as Tab. I but for SLS and ALS represented by the three range Gaussian forms given in Eq. (3).

c	i	1	2	3
	β_i	0.40	0.80	1.20
SLS	$a_i^{(SLS)}$	-12920.0	372.4	-2.030
	$b_i^{(SLS)}$	24580.0	-840.0	0.0
	$c_i^{(SLS)}$	-10180.0	337.1	0.0
ALS	$a_i^{(ALS)}$	1985.0	12.73	2.109
	$b_i^{(ALS)}$	-1828.0	41.30	0.0
	$c_i^{(ALS)}$	679.8	-17.58	0.0

among the ground-state spin-doublet splittings in hypernuclei that are obtained on the shell model basis, rather independently of the other sections. Then, secondly, we will show the share of odd-state interaction components in these doublets also in a schematic way without entering into detailed forms of the ΛN interactions.

Noting that the typical hypernuclei such as $^{10}_\Lambda\text{Be}$, $^{10}_\Lambda\text{B}$, $^{11}_\Lambda\text{B}$, $^{12}_\Lambda\text{B}$, and $^{12}_\Lambda\text{C}$ are dominantly of spherical nature, we take a schematic prescription specifically in this section. Here we take the L - S coupling shell model scheme and assume that each ground state of the corresponding nuclear core (J_c, T_c) is described by an $SU(3)$ configuration [32, 33] with maximum orbital symmetry, denoted by $[f](\lambda, \mu)$. Then hypernuclear spin-doublet wave functions $\Psi_A(J = J_c \pm \frac{1}{2})$ for $^{10}_\Lambda\text{Be}(J = 1^-, 2^-)$, $^{11}_\Lambda\text{B}(5/2^+, 7/2^+)$, and $^{12}_\Lambda\text{B}(1^-, 2^-)$, are described respectively as

$$\begin{aligned} & \{^9\text{Be}; p^5[41](31)_{L=1}(S = \frac{1}{2}, T_c = \frac{1}{2}), J_c = 3/2^-_g\} \times s^{\Lambda}_{1/2}, \\ & \{^{10}\text{B}; p^6[42](22)_{L=2}(S = 1, T_c = 0), J_c = 3^+_g\} \times s^{\Lambda}_{1/2}, \\ & \{^{11}\text{B}; p^7[41](31)_{L=1}(S = \frac{1}{2}, T_c = \frac{1}{2}), J_c = 3/2^-_g\} \times s^{\Lambda}_{1/2}. \end{aligned}$$

The analogous wave functions are given for $^{10}_\Lambda\text{B}(1^-, 2^-)$ and $^{12}_\Lambda\text{C}(1^-, 2^-)$, respectively. Hereafter T_c is implicit, as the Λ isospin is zero.

In order to estimate the hypernuclear doublet energy splitting, the total ΛN interaction energy defined by

$$E_A(J = J_c \pm \frac{1}{2}) \equiv \langle \Psi_A(J) | \sum_i V_{N\Lambda}(i, 1) | \Psi_A(J) \rangle \quad (10)$$

is calculated analytically within the full p -shell L - S coupling model space. The resultant total energy is expressed in terms of the ΛN two-body interaction matrix elements in the jj -coupling instead of the L - S coupled one $\langle p^N s^\Lambda(L) S | v | p^N s^\Lambda(L') S' \rangle_{J'}$, because here we intend to show the share of $p_{3/2}$ and $p_{1/2}$ contributions. For this purpose, we use the following simplified notations.

$$\begin{aligned} V_3(J') & \equiv \langle p^N_{3/2} s^\Lambda_{1/2} | v | p^N_{3/2} s^\Lambda_{1/2} \rangle_{J'=1^-, 2^-}, \\ V_1(J') & \equiv \langle p^N_{1/2} s^\Lambda_{1/2} | v | p^N_{1/2} s^\Lambda_{1/2} \rangle_{J'=0^-, 1^-}, \\ V_{31}(J') & \equiv \langle p^N_{3/2} s^\Lambda_{1/2} | v | p^N_{1/2} s^\Lambda_{1/2} \rangle_{J'=1^-}. \end{aligned} \quad (11)$$

For the interaction energies $E_{10}(J)$ of $^{10}_\Lambda\text{Be}(1^-, 2^-)$, the

detailed calculation leads to the following expressions:

$$\begin{aligned} E_{10}(1^-) & = \frac{48}{45} V_3(2^-) + \frac{5}{9} V_3(1^-) + \frac{5}{9} V_1(1^-) \\ & + \frac{1}{3} V_1(0^-) - \frac{9\sqrt{2}}{5} V_{31}(1^-), \end{aligned} \quad (12)$$

$$\begin{aligned} E_{10}(2^-) & = \frac{501}{225} V_3(2^-) + \frac{16}{25} V_3(1^-) + \frac{37}{25} V_1(1^-) \\ & + \frac{147}{225} V_1(0^-) + \frac{27\sqrt{2}}{25} V_{31}(1^-). \end{aligned} \quad (13)$$

Then we get the doublet energy splitting ΔE_{10} as

$$\begin{aligned} \Delta E_{10}(2^- - 1^-) & = \frac{29}{25} \{V_3(2^-) - V_3(1^-)\} \\ & + \frac{8}{25} \{V_1(0^-) - V_1(1^-)\} + \frac{72\sqrt{2}}{25} V_{31}(1^-). \end{aligned} \quad (14)$$

The energies of $^{12}_\Lambda\text{B}(1^-, 2^-)$ are obtained as follows:

$$\begin{aligned} E_{12}(1^-) & = \frac{149}{60} V_3(2^-) + \frac{53}{20} V_3(1^-) + \frac{8}{5} V_1(1^-) \\ & + \frac{4}{15} V_1(0^-) - \frac{9\sqrt{2}}{5} V_{31}(1^-), \end{aligned} \quad (15)$$

$$\begin{aligned} E_{12}(2^-) & = \frac{1093}{300} V_3(2^-) + \frac{149}{100} V_3(1^-) + \frac{32}{25} V_1(1^-) \\ & + \frac{44}{75} V_1(0^-) + \frac{27\sqrt{2}}{25} V_{31}(1^-). \end{aligned} \quad (16)$$

As a result of the difference $E_{12}(2^-) - E_{12}(1^-)$, it is quite interesting to obtain exactly the same energy splitting of ΔE_{12} for $^{12}_\Lambda\text{B}$ as that for $^{10}_\Lambda\text{Be}$ given by Eq.(14). Thus we can write

$$\Delta E_{12}(2^- - 1^-) = \Delta E_{10}(2^- - 1^-). \quad (17)$$

The doublet energies for $^{11}_\Lambda\text{B}(5/2^+, 7/2^+)$ are obtained in the similar way as

$$\begin{aligned} E_{11}(5/2^+) & = \frac{25}{18} V_3(2^-) + \frac{8}{3} V_3(1^-) + \frac{31}{18} V_1(1^-) \\ & + \frac{5}{18} V_1(0^-) - \frac{16\sqrt{2}}{9} V_{31}(1^-), \end{aligned} \quad (18)$$

$$\begin{aligned} E_{11}(7/2^+) & = \frac{10}{3} V_3(2^-) + \frac{3}{3} V_3(1^-) + \frac{4}{3} V_1(1^-) \\ & + \frac{2}{3} V_1(0^-) + \frac{12\sqrt{2}}{9} V_{31}(1^-). \end{aligned} \quad (19)$$

Therefore the doublet energy splitting ΔE_{11} is given by

$$\begin{aligned} \Delta E_{11}(7/2^+ - 5/2^+) & = \frac{35}{18} \{V_3(2^-) - V_3(1^-)\} \\ & + \frac{7}{18} \{V_1(0^-) - V_1(1^-)\} + \frac{28\sqrt{2}}{9} V_{31}(1^-). \end{aligned} \quad (20)$$

We have two experimental energy splittings so far [34, 35] among the adjacent hypernuclei concerned here:

$$\Delta E(^{12}_\Lambda\text{C}; 2^- - 1^-)^{\text{exp}} = 0.162 \text{ MeV}, \quad (21)$$

$$\Delta E(^{11}_\Lambda\text{B}; 7/2^+ - 5/2^+)^{\text{exp}} = 0.263 \text{ MeV}. \quad (22)$$

If we compare the leading terms of Eq.(20) and Eq.(17), we get the ratio $\Delta E_{11}/\Delta E_{12} \simeq (\frac{35}{18})/(\frac{29}{25}) \simeq 1.67$, since the remaining terms amount to much smaller contributions. This theoretical ratio is in very good agreement with the experimental ratio (1.62). This fact manifests certain applicability of the present prescription based on

the SU(3) classification. Thus, on the basis of the relation obtained by Eq.(17), we firmly predict the unknown energy splittings between the spin-doublet states as

$$\Delta E({}^{10}_{\Lambda}\text{Be}) \simeq \Delta E({}^{10}_{\Lambda}\text{B}) \simeq \Delta E({}^{12}_{\Lambda}\text{B}) \simeq \Delta E({}^{12}_{\Lambda}\text{C})^{\text{exp}}. \quad (23)$$

In the recent ${}^{12}\text{C}(e, e'K^+){}^{12}_{\Lambda}\text{B}$ experiment, a spectroscopic analysis of the lowest peak shape has been made, suggesting $\Delta E({}^{12}_{\Lambda}\text{B}) \simeq 0.18$ MeV [36], which is well compared with $\Delta E({}^{12}_{\Lambda}\text{C})^{\text{exp}}$ and is also consistent with a theoretical prediction of the energies and cross sections [37].

In the actual calculations with the HyperAMD framework, as shown in the next section, the results depend on the detailed realistic structures such as hypernuclear deformation and density distribution. Nevertheless the basic relations mentioned above give a useful insight into these hypernuclear structures.

Second, it is also interesting to see the contribution from relative odd-state interactions to the doublet splitting. By expanding the two-body interaction matrix elements in terms of the relative and CM coordinates, the splitting energy for the case of ΔE_{10} is reexpressed as

$$\begin{aligned} & \Delta E_{10}(2^- - 1^-_g) \\ &= \frac{7}{5} \langle 0\tilde{s} | V^{(3E)}(r) | 0\tilde{s} \rangle + \frac{13}{15} \langle 0\tilde{s} | V^{(1E)}(r) | 0\tilde{s} \rangle \\ &- \frac{2}{5} \langle 0\tilde{p} | V^{(3O)}(r) | 0\tilde{p} \rangle + \frac{13}{15} \langle 0\tilde{p} | V^{(1O)}(r) | 0\tilde{p} \rangle \\ &+ \frac{72\sqrt{2}}{75} \langle 0\tilde{p}(S_0) | V^{(ALS)}(r) | 0\tilde{p}(S_1) \rangle_{\mathcal{I}=1}. \quad (24) \end{aligned}$$

Here $0\tilde{s}$ and $0\tilde{p}$ denote the relative radial states of ΛN two-body system with the spin coupling ($\mathbf{l} + \mathbf{S} = \mathbf{I}$). Each central potential $V^{(c)}(r)$ is given by sum of the corresponding terms defined by Eqs.(2) - (4), although in the above expression the SLS spin-orbit component is formally included in the $\langle 0\tilde{p} | V^{(3O)}(r) | 0\tilde{p} \rangle$ part. Equation (24) shows clearly that, in addition to the relative \tilde{s} -state interactions, the \tilde{p} -state central interactions and the SLS/ALS interactions contribute in this way to the p -shell hypernuclear doublet splitting. In this respect it is interesting to compare the expression of Eq.(24) with that for the doublet splitting in ${}^4_{\Lambda}\text{H}$ in the lowest configuration:

$$\begin{aligned} & \Delta E_4(1^+ - 0^+_g) \\ &\equiv E({}^4_{\Lambda}\text{H}; 1^+) - E({}^4_{\Lambda}\text{H}; 0^+_g) \\ &= \langle 0\tilde{s} | V^{(3E)}(r) | 0\tilde{s} \rangle - \langle 0\tilde{s} | V^{(1E)}(r) | 0\tilde{s} \rangle, \quad (25) \end{aligned}$$

where only the even-state interactions work. Also we note that the oscillator size (b) for s -shell hypernuclei is implicit and it is different from the p -shell cases. It should be noted that, in actual calculations, the even- and odd-state combinations of ΛN spin-dependent interactions are determined carefully within the freedom as prescribed by Eq. (5), *i.e.* the contributions of the even- and odd-state components can be different from those

given by Eq. (24) due to dynamical effects such as nuclear deformations and/or density dependence of the ΛN interaction, which are fully taken into account in the HyperAMD calculation using Eq. (5) as presented in the following section.

IV. NUMERICAL RESULTS AND DISCUSSIONS

In this section, we discuss low-lying level structure affected by ΛN spin-spin and spin-orbit interactions. In Ref. [25], the spin orderings of the ground-state doublet are inconsistent with the observations in ${}^{10}_{\Lambda}\text{B}$, ${}^{11}_{\Lambda}\text{B}$, ${}^{12}_{\Lambda}\text{B}$, ${}^{12}_{\Lambda}\text{C}$, ${}^{15}_{\Lambda}\text{N}$, and ${}^{16}_{\Lambda}\text{O}$, where the HyperAMD calculations were performed using the ΛN central force derived from ESC14+MBE but without the ΛN spin-orbit force. These behaviors would be caused by the properties of the ΛN spin-spin force and/or absence of the ΛN spin-orbit force. In this paper, we focus on the spin-spin and spin-orbit splittings in ${}^7_{\Lambda}\text{Li}$, ${}^9_{\Lambda}\text{Li}$, ${}^9_{\Lambda}\text{Be}$, ${}^{10}_{\Lambda}\text{Be}$, ${}^{10}_{\Lambda}\text{B}$, ${}^{11}_{\Lambda}\text{B}$, ${}^{12}_{\Lambda}\text{C}$, ${}^{13}_{\Lambda}\text{C}$, ${}^{15}_{\Lambda}\text{N}$, and ${}^{16}_{\Lambda}\text{O}$.

A. Excitation spectra of core nuclei

In this study, the excitation spectra of hypernuclei are compared with those of the core nuclei and observed data of the hypernuclei. Since the experimental information of hypernuclei is concentrated in the energy regions near the ground states, it is quite important to describe the low-lying spectra of the core nuclei properly before the discussion of the hypernuclei.

We perform the antisymmetrized molecular dynamics (AMD) calculation for ${}^6\text{Li}$, ${}^8\text{Li}$, ${}^8\text{Be}$, ${}^9\text{Be}$, ${}^9\text{B}$, ${}^{10}\text{B}$, ${}^{11}\text{C}$, ${}^{12}\text{C}$, ${}^{14}\text{N}$, and ${}^{15}\text{O}$ using the original parameter set of Gogny D1S given in Refs. [29, 30]. These nuclei have various structure. For example, in ${}^8\text{Be}$ and ${}^9\text{Be}$, it is well known that 2α clustering is dominated near the ground states, whereas the ground state $3/2^-$ of ${}^{15}\text{O}$ is well understood by a neutron one-hole configuration in the shell-model picture. In ${}^{12}\text{C}$, the ground state has a mixed nature of the 3α cluster and shell-model like structures [38–43].

First, we discuss the excitation spectra of the nuclei other than ${}^8\text{Be}$, ${}^9\text{Be}$ and ${}^9\text{B}$, namely ${}^6\text{Li}$, ${}^8\text{Li}$, ${}^9\text{B}$, ${}^{10}\text{B}$, ${}^{11}\text{C}$, ${}^{12}\text{C}$, ${}^{14}\text{N}$, and ${}^{15}\text{O}$, which are shown in Fig. 1. It is found that the present AMD calculation successfully reproduces the spin-parity of the ground states. The low-lying states in these nuclei are obtained with correct ordering except for ${}^8\text{Li}$. It is noted that the 1^+ state of ${}^8\text{Li}$ is also obtained at 5.27 MeV, which is higher than the 3^+ state. In ${}^{12}\text{C}$, since the AMD model can describe both the cluster and shell-model like structures, we obtain a reasonable value of the excitation energy of the 2^+ state, which is sensitive to the mixed nature of the ground state mentioned above.

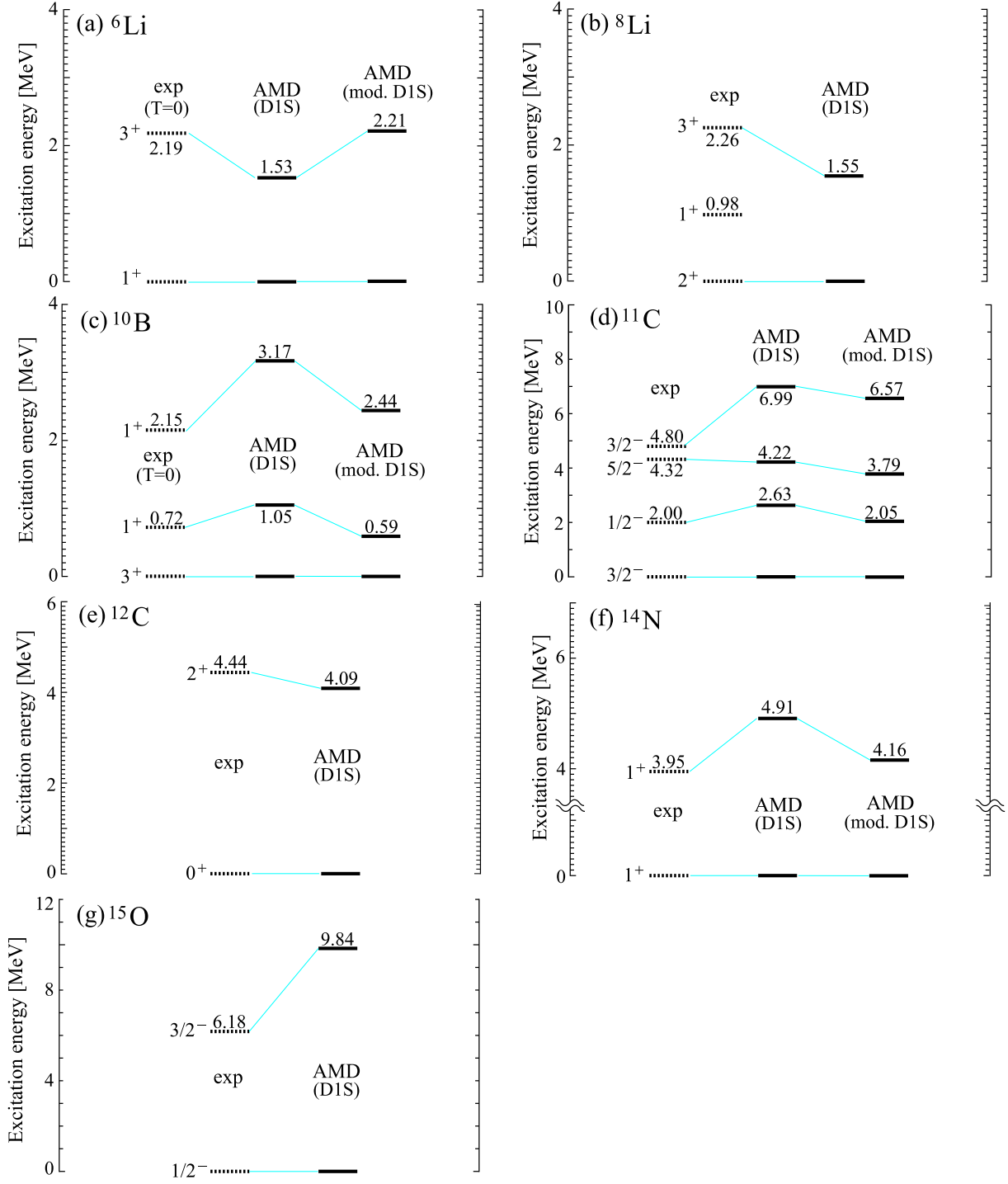


FIG. 1: Calculated and observed excitation spectra of the core nuclei ${}^6\text{Li}$, ${}^8\text{Li}$, ${}^{10}\text{B}$, ${}^{12}\text{C}$, ${}^{13}\text{C}$, ${}^{14}\text{N}$, and ${}^{15}\text{O}$. Numbers shown in the spectra are excitation energies [MeV]. In panels (a), (b), (c), (d) and (f), the calculated results with the Gogny D1S modified so as to reproduce $Ex({}^6\text{Li}; 3^+)$ (mod. D1S) are shown together with those with the original parameter set of the Gogny D1S (D1S). The observed data are taken from Ref. [45] for ${}^6\text{Li}$, Ref. [46] for ${}^{11}\text{C}$, Ref. [47] for ${}^{12}\text{C}$, Ref. [48] for ${}^{14}\text{N}$ and ${}^{15}\text{O}$, and Ref. [49] for the others.

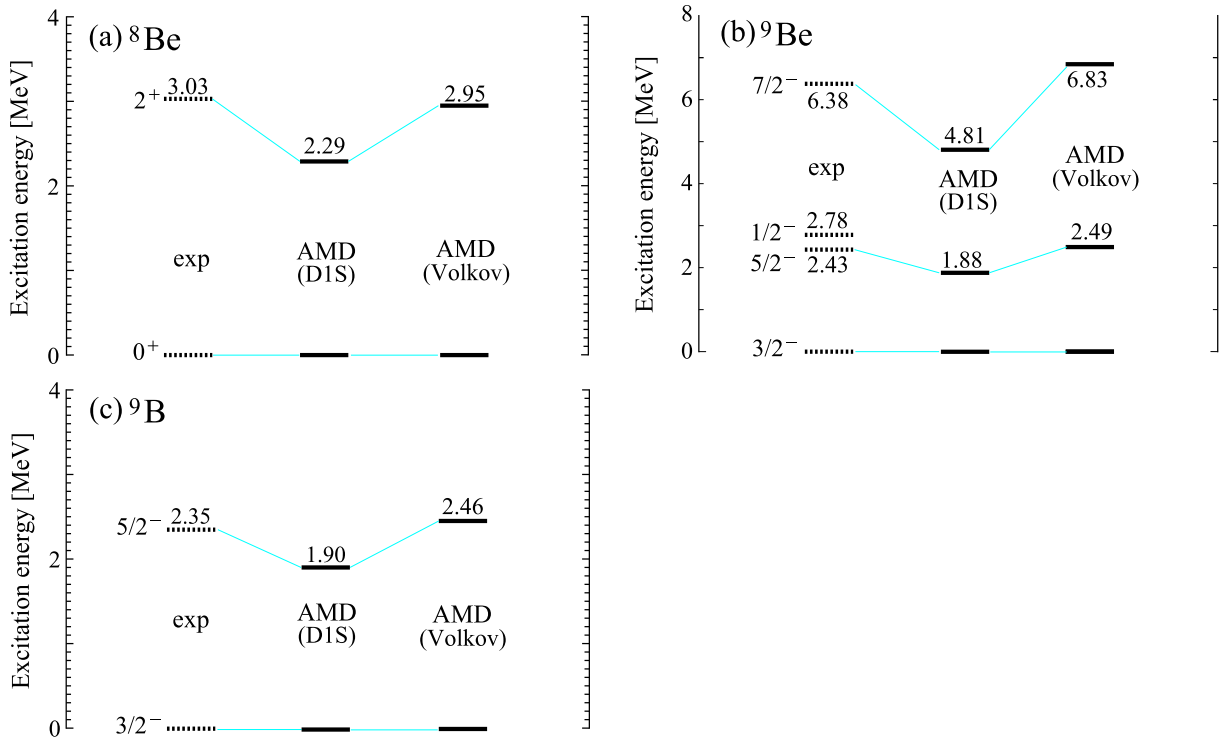


FIG. 2: Same as Fig.1 but for ${}^8\text{Be}$, ${}^9\text{Be}$ and ${}^9\text{B}$. The calculated results with Volkov No.2 (Volkov) are compared with those with Gogny D1S (D1S). The observed data are taken Ref. [49].

Though the AMD calculation reproduces the gross features of the nuclei such as the level ordering, we see deviations of the calculated excitation energies from the experimental data. For example, in ${}^6\text{Li}$, the excitation energy of 3^+ , $E_x({}^6\text{Li}; 3^+)$, is lower than the experimental data by about 700 keV, which is quite important because the coupling of a Λ particle to this state generates an experimentally well-known spin doublet ($5/2^+$, $7/2^+$) in ${}^7_\Lambda\text{Li}$. In the other nuclei, we see the deviation of the excitation energies from the observed data by about several hundred keV or more. For the quantitative discussions of the hypernuclei, these deviations should be improved as possible.

Here, we try to modify the parameters of Gogny D1S so as to reproduce the $E_x({}^6\text{Li}; 3^+)$ value. The central force of the Gogny D1S is given by the two-range Gaussian form as

$$V_{NN}^{\text{cent}} = \sum_{i=1}^2 \exp[-(r/\beta_i)^2] \times \{W_i + B_i \hat{P}_\sigma - H_i \hat{P}_\tau - M_i \hat{P}_\sigma \hat{P}_\tau\}, \quad (26)$$

where \hat{P}_σ and \hat{P}_τ are the spin and isospin exchange operators, respectively. In general, varying the parameters B_i and H_i controls the ratio of the 3E interaction to the 1E interaction with keeping the sum of W_i and M_i . Since these parameters can be changed depending on each nuclear system, we modify B_i and H_i for the

both ranges ($i = 1, 2$) by multiplying a common factor α^{NN} so as to reproduce the $E_x({}^6\text{Li}; 3^+)$ value, while the W_i and M_i are unchanged from the original values of the Gogny D1S. As a result, we find that the $\alpha^{NN} = 1.2$ gives $E_x({}^6\text{Li}; 3^+) = 2.21$ MeV, which is much close to the observed value $E_x^{\text{exp}}({}^6\text{Li}; 3^+) = 2.19$ MeV. It is also found that this modification improves the excitation spectra of ${}^{10}\text{B}$, ${}^{11}\text{C}$, and ${}^{14}\text{N}$ as shown in Fig. 1 except for the $3/2^-$ state of ${}^{11}\text{C}$. On the other hand, in ${}^{15}\text{O}$, the excitation energy of the $3/2^-$ state is largely different from the observed value. We consider that this difference mainly comes from the description of neutron single-particle orbits, because the $3/2^-$ state is generated by a neutron from $0p_{3/2}$ to $0p_{1/2}$ in a naive shell-model picture.

In Fig. 2, we show the excitation spectra of ${}^8\text{Be}$, ${}^9\text{Be}$ and ${}^9\text{B}$, which are characterized by having the 2α , $2\alpha + n$ and $2\alpha + p$ cluster structure, respectively. It is found that the present calculation with Gogny D1S reproduces the level ordering except for the $1/2^-$ state in ${}^9\text{Be}$ and ${}^9\text{B}$. However, the excitation energies are slightly lower than the experimental data in ${}^8\text{Be}$, ${}^9\text{Be}$ and ${}^9\text{B}$. Since they have the well-developed 2α cluster structure, it is considered that the difference of the excitation energies shows the overestimation of the momentum of inertia of the 2α clustering. In general, a density-dependent interaction tends to overestimate the nuclear clustering, because it works as a repulsive force when the nuclear density is increased in cluster states. Since the degree

of the 2α clustering as well as the size of the α particle affect the momentum of inertia, the difference of the excitation energies in Fig. 2 would be caused by the density-dependent interaction of Gogny D1S. Instead of the Gogny D1S, we use the Volkov No. 2 force [31] together with the spin-orbit force of the G3RS interaction [44] for ${}^8\text{Be}$, ${}^9\text{Be}$ and ${}^9\text{B}$ (see Fig. 2). The Volkov No. 2 is one of the effective nuclear forces often used in the structure studies on α cluster structure, which does not have the density-dependent term as given by

$$V_{NN}^{\text{cent}} = \sum_{i=1}^2 v_i \exp[-(r/\beta_i)^2] \times \{(1.0 - m) + bP_\sigma - hP_\tau - mP_\sigma P_\tau\}. \quad (27)$$

Here, the parameters are fixed to be $m = 0.60$ and $b = h = 0.125$. The strength of the spin-orbit force of the G3RS is fixed to be 1600 MeV. In Fig. 2(a), in ${}^8\text{Be}$, we see that the excitation energy of the 2^+ state becomes 2.95 MeV with Volkov No. 2, which is close to the experimental value ($E_x^{\text{exp}}({}^8\text{Be}; 2^+) = 3.03$ MeV). The energy spectra of ${}^9\text{Be}$ and ${}^9\text{B}$ are also improved as shown in Fig. 2(b)-(c).

We also give a comment on the $1/2^-$ state in ${}^9\text{Be}$ and ${}^9\text{B}$, which are missing in Fig. 2(b)-(c). This is caused by the procedure of the variational calculation. In $1/2^-$ state of ${}^9\text{Be}$, the last neutron occupies the $p_{1/2}$ orbit in the $2\alpha + n$ cluster model picture. In the present calculation, the nucleon configuration is determined by the energy variation performed before the angular momentum projection. As a result, the last neutron mainly occupies the $p_{3/2}$ orbit than the $p_{1/2}$ orbit. In ${}^9\text{B}$, which is the mirror nucleus of ${}^9\text{Be}$, the $1/2^-$ state does not appear because the last proton occupies the $p_{3/2}$ orbit as the results of the energy variation.

From the above results, we use the modified version of the Gogny D1S as the effective nuclear interaction in the HyperAMD calculation for ${}^7_\Lambda\text{Li}$, ${}^{11}_\Lambda\text{B}$, ${}^{12}_\Lambda\text{C}$, and ${}^{15}_\Lambda\text{N}$, whereas the original parameter set of it is employed for ${}^9_\Lambda\text{Li}$, ${}^{13}_\Lambda\text{C}$, and ${}^{16}_\Lambda\text{O}$. In ${}^9_\Lambda\text{Be}$, ${}^{10}_\Lambda\text{Be}$ and ${}^{10}_\Lambda\text{B}$, the Volkov No.2 force is used together with the spin-orbit force of the G3RS instead of Gogny D1S.

B. Tuning of spin-dependent ΛN interaction

Let us move to the discussions on the hypernuclei. In this section, we tune the ΛN spin-spin and spin-orbit interactions in light Λ hypernuclei. First, we focus on the spin doublet (0^+ , 1^+) of ${}^4_\Lambda\text{H}$ generated by the coupling of a Λ particle to the $1/2^+$ state of ${}^3\text{H}$, where the even-state spin-spin force v_σ^E dominantly acts between each nucleon and the Λ particle in s orbit. In Fig. 3(a), we show the calculated result of ${}^4_\Lambda\text{H}$ with the original parameter sets of Gogny D1S and ESC14+MBE as the effective nuclear and ΛN interactions, respectively. Here we use the k_F value which reproduces the B_Λ^{exp} value of ${}^4_\Lambda\text{H}$, namely $k_F = 0.95 \text{ fm}^{-1}$ ($k_F = 0.93 \text{ fm}^{-1}$) giving $B_\Lambda = 2.09 \text{ MeV}$

($B_\Lambda = 2.14 \text{ MeV}$) with (without) tuning. It is seen that the excitation energy of the 1^+ state is slightly underestimated (0.97 MeV) in comparison with the observed value ($E_x^{\text{exp}}({}^4_\Lambda\text{H}; 1^+) = 1.09 \pm 0.02 \text{ MeV}$). Here we tune the even-state spin-spin force v_σ^E by adding a correction term ΔV^E to the 2nd range as

$$\Delta V^E \exp[-(r/\beta_2)^2] \vec{\sigma} \cdot \vec{\sigma} P(E). \quad (28)$$

As a result, the experimental value $E_x^{\text{exp}}({}^4_\Lambda\text{H}; 1^+)$ is reproduced by using $\Delta V^E = 1.2 \text{ MeV}$ as shown in the middle of Fig. 3(a).

To tune the odd-state spin-spin force v_σ^O , we focus on the excitation spectra of ${}^7_\Lambda\text{Li}$, where the spin doublets ($1/2^+$, $3/2^+$) and ($5/2^+$, $7/2^+$) are observed corresponding to the 1^+ and 3^+ states of ${}^6\text{Li}$, respectively. One can consider that ${}^6\text{Li}$ has the cluster structure composed of the spin-saturated α particle and the d cluster with spin 1, the relative angular momentum between α and d is zero $l = 0$ in the ground state 1^+ , whereas the 3^+ state is generated by the coupling of $l = 2$ and spin 1 of d . In ${}^7_\Lambda\text{Li}$, the spin-spin forces in both even and odd parity states contribute to the ($1/2^+$, $3/2^+$) and ($5/2^+$, $7/2^+$). It is noted that the ΛN spin-orbit force acts only in the ($5/2^+$, $7/2^+$) state, because the Λ particle mainly occupies the s orbit in ${}^7_\Lambda\text{Li}$. Here, we calculate the lowest doublet ($1/2^+$, $3/2^+$) using the ESC14+MBE with $\Delta V^E = 1.2 \text{ MeV}$ as shown in Fig. 3(b), where the result with the original parameter set of ESC14+MBE is also shown. It is seen that the excitation energy of $3/2^+$ is increased by adding $\Delta V^E = 1.2 \text{ MeV}$ (0.52 MeV), but still lower than the experimental value (0.69 MeV). In the same manner as the even-state spin-spin force, we add the correction term ΔV^O as

$$\Delta V^O \exp[-(r/\beta_2)^2] \vec{\sigma} \cdot \vec{\sigma} P(O), \quad (29)$$

to the odd-state spin-spin force and determine $\Delta V^O = 30.0 \text{ MeV}$ for reproducing $E_x({}^7_\Lambda\text{Li} : 3/2^+)$ (see the 3rd from the left in Fig. 3(b)). Since ΔV^E and ΔV^O are k_F independent, one can renormalize these corrections into $a_i^{(c)}$ in Eq. (3) using the relation among Eqs. (2) - (5). The corrected parameters $a_i^{(c)}$ for Eq. (3) are shown in parenthesis in Tab. I.

In addition to the spin-spin force, we also modify the ΛN spin-orbit force so as to reproduce the energy splitting between $3/2^+$ and $5/2^+$ of ${}^9_\Lambda\text{Be}$. Since ${}^8\text{Be}$ has well pronounced 2α cluster structure, the 1st excited state 2^+ is mainly generated by the relative angular momentum $l = 2$ between 2α . If a Λ particle is injected to this state, the energy splitting between $3/2^+$ and $5/2^+$ is mainly caused by the ΛN spin-orbit force. In ${}^9_\Lambda\text{Be}$, using the original SLS and ALS force, the energy splitting between the $3/2^+$ and $5/2^+$ states is 150 keV, which is much larger than the experimental value (40 keV). It is well known that the spin-orbit splitting by the ΛN interaction is quite small compared with that by nuclear force, which is due to the large cancellation between SLS and ALS forces. Therefore, we strengthen the ALS by multiplying

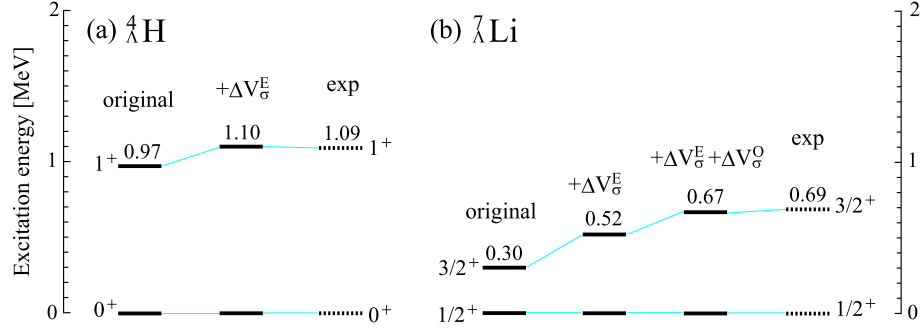


FIG. 3: (a) Comparison of calculated (solid) and observed (dotted) excitation spectra of ${}^4_\Lambda\text{H}$. Calculated spectrum with the original parameter set of ESC14+MBE is shown in the left (original), while that using ESC14+MBE with tuning the ΛN even-state spin-spin force is shown in the middle ($+\Delta V_\sigma^E$). Numbers shown in the spectra are excitation energies [MeV]. (b) Same as (a) but for ${}^7_\Lambda\text{Li}$. Calculated spectrum using ESC14+MBE with the tuning in the ΛN even-state (even and odd state) spin-spin force(s) are shown in the 2nd (3rd) from the left, while that without tuning is displayed in the left. Experimental data are taken from Refs. [50–53].

a factor α_{ALS} to make the cancellation larger with keeping the strength of the SLS. It is found that the energy spacing between $3/2^+$ and $5/2^+$ becomes smaller as the α_{ALS} increases. As a result, we determine $\alpha_{\text{ALS}} = 1.9$, which gives the splitting energy of 60 keV.

Hereafter we use the ΛN central force of ESC14+MBE with both $\Delta V^E = 1.2$ MeV and $\Delta V^O = 30.0$ MeV as well as the ΛN spin-orbit force with $\alpha_{\text{ALS}} = 1.9$.

C. Ground-state spin of the hypernuclei

Using the ΛN interaction tuned in Sec. IV B, we apply the HyperAMD to the p shell hypernuclei, ${}^7_\Lambda\text{Li}$, ${}^9_\Lambda\text{Li}$, ${}^9_\Lambda\text{Be}$, ${}^{10}_\Lambda\text{Be}$, ${}^{10}_\Lambda\text{B}$, ${}^{11}_\Lambda\text{B}$, ${}^{12}_\Lambda\text{C}$, ${}^{13}_\Lambda\text{C}$, ${}^{15}_\Lambda\text{N}$, and ${}^{16}_\Lambda\text{O}$, which are shown in Fig. 4.

Since the YNG interaction depends on the nuclear density through the Fermi momentum k_F , it is necessary to select the k_F properly in each system. In this paper, except for ${}^7_\Lambda\text{Li}$, ${}^9_\Lambda\text{Li}$, ${}^9_\Lambda\text{Be}$, ${}^{10}_\Lambda\text{Be}$ and ${}^{10}_\Lambda\text{B}$, we use the same k_F values as in Ref. [25] determined under the ADA, where the k_F values are obtained from the densities of the nucleons (ρ_N) and Λ particle (ρ_Λ), as

$$k_F = \left(\frac{3\pi^2 \langle \rho \rangle}{2} \right)^{1/3}, \quad \langle \rho \rangle = \int d^3r \rho_N(\mathbf{r}) \rho_\Lambda(\mathbf{r}). \quad (30)$$

The k_F values used are listed in Tab. III, where the common k_F value is used for the ground and excited states in each hypernucleus. The Λ binding energy B_Λ is also shown in Tab. III, which is defined by the energy gain of a hypernuclear state from the corresponding state in the core nucleus. It is found that the B_Λ values are increased compared with those in Ref. [25], and thus are larger than the observed values (B_Λ^{exp}). For example, in ${}^{12}_\Lambda\text{C}$, the B_Λ is 12.28 MeV in Tab. III, whereas $B_\Lambda = 11.0$ MeV in Ref. [25]. This is mainly due to the inclusion of the ΛN spin-orbit force. Since the ADA given by Eq.(30) is one of the methods to obtain reasonable values of k_F

from the structure calculation, there is a room to modify the ADA to reproduce B_Λ^{exp} . For example, in Ref. [25], the authors (M.I and Y.Y) introduced a small correction parameter in Eq. (30) for the p -states of several Λ hypernuclei. In the same way, it is possible to modify the ADA using a small correction parameter in the present calculation. In ${}^7_\Lambda\text{Li}$, ${}^9_\Lambda\text{Li}$, ${}^9_\Lambda\text{Be}$ and ${}^{10}_\Lambda\text{Be}$, the k_F values are determined so as to reproduce the observed values of the B_Λ in the ground states. This is because the HyperAMD with the ADA treatment largely overestimates the B_Λ values in the light hypernuclei ($A < 10$) and/or the hypernuclei with α clustering as pointed out in Ref. [25].

Let us discuss the spin-parity of the ground states of the hypernuclei. In Fig. 4, the excitation spectra of the hypernuclei are compared with those of the core nuclei and experimental data. It shows that the calculation successfully reproduces the level ordering of the ground-state doublets of ${}^7_\Lambda\text{Li}$, ${}^{10}_\Lambda\text{B}$, ${}^{11}_\Lambda\text{B}$, ${}^{12}_\Lambda\text{C}$, and ${}^{15}_\Lambda\text{N}$, in which incorrect spin was obtained for the ground states in Ref. [25]. The difference of the calculations between Ref. [25] and this paper is the ΛN interaction, namely tuning of the spin-spin force and inclusion of the spin-orbit force, which improves the incorrect ordering of the spin doublet partners. In ${}^{16}_\Lambda\text{O}$, the degenerated ground state doublet is obtained in the calculation, though the ground-state spin is different with the observed one. Thus the ΛN spin-spin and spin-orbit interactions are essential to describe the ground state spin properly.

We predict the ground-state spin and parity of ${}^9_\Lambda\text{Li}$ and ${}^{10}_\Lambda\text{Be}$, which are not measured by experiments. In ${}^9_\Lambda\text{Li}$, Figure 4 (b) shows that the $3/2^+$ state is lower than the $5/2^+$ state in the ground-state doublet, which is opposite to the prediction in Ref. [25] where the $5/2^+$ state is predicted to be the ground state. Similarly, in Fig. 4(d), the 1^- states is predicted as the ground states of ${}^{10}_\Lambda\text{Be}$, whereas the 2^- is the lowest in Ref. [25]. From the above discussion, we consider that the ground-state spin predicted by the present work is more reliable than

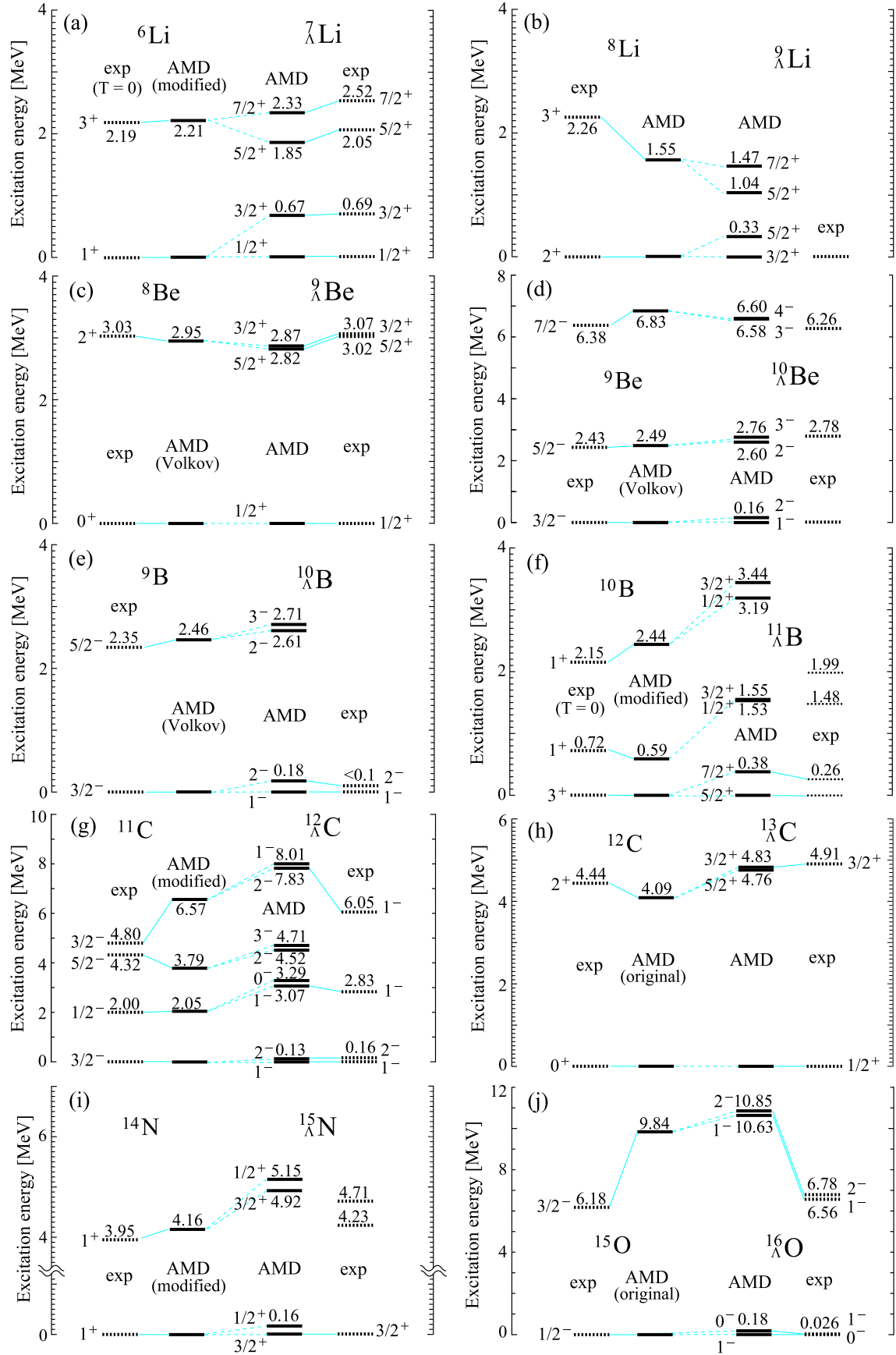


FIG. 4: Calculated (solid) and observed (dotted) excitation spectra. Numbers shown in the spectra are excitation energies [MeV]. Observed data of the excitation spectra are also shown for ${}^7\text{Li}$ [52, 53], ${}^9\text{Be}$ [54], ${}^{10}\text{Be}$ [55], ${}^{10}\text{B}$ [56, 57], ${}^{11}\text{B}$ [34], ${}^{12}\text{C}$ [35], ${}^{13}\text{C}$ [1, 58], ${}^{15}\text{N}$ [56], and ${}^{16}\text{O}$ [59].

that in Ref. [25]. Furthermore, it is also found that the above tuning of ESC14+MBE reproduces the observed ground-state spin of ${}_{\Lambda}^{19}\text{F}$. The detailed result of ${}_{\Lambda}^{19}\text{F}$ will be reported in a forthcoming paper.

D. Comparison of the excitation spectra with the experimental data

In this section, we discuss not only the ground states but also the excited states of each hypernuclei in detail in comparison with the observed data.

In ${}_{\Lambda}^7\text{Li}$, it is found that both of the splitting and excitation energies of the $(5/2^+, 7/2^+)$ doublet are almost consistent with the experimental data. In particular, the splitting energy of this doublet is important to test the tuned ΛN interaction, where the ΛN spin-orbit force also affects in addition to the even and odd state spin-spin force. This is because the core state 3^+ of ${}^6\text{Li}$ is generated by the coupling of the relative angular momentum $l = 2$ between α and d and the spin 1 of the d in a naive $\alpha + d$ cluster model picture. In Fig. 4, the splitting energy of the $(5/2^+, 7/2^+)$ doublet is 0.48 MeV, which is almost the same as the observed value (0.47 MeV), whereas that is 0.33 MeV if the original parameter set of the ΛN spin-orbit interaction is used. Thus the energy splitting of the $(5/2^+, 7/2^+)$ doublet is consistently obtained by the tuning of the ΛN spin-orbit interaction in ${}_{\Lambda}^9\text{Be}$ in Sec. IV B.

In the other hypernuclei, the excitation spectra are successfully described using the ΛN interaction tuned in Sec. IV B. In ${}_{\Lambda}^{10}\text{B}$, the energy splitting of the ground-state doublet is small (0.18 MeV). In ${}_{\Lambda}^{13}\text{C}$, the excitation energy of the $3/2^+$ is consistent with that measured by the γ -ray spectroscopy experiment. In ${}_{\Lambda}^{10}\text{Be}$, the excitation energies of the $(2_2^-, 3_1^-)$ and $(3_2^-, 4^-)$ doublets are consistent with the excited states observed at 2.78 MeV and 6.26 MeV with unknown spin-parity. In ${}_{\Lambda}^{11}\text{B}$, the present calculation almost reproduces the energy spacing of the observed ground-state doublet. It is found that the contribution from the odd-state spin-spin interaction is quite small in the ground-state doublet of ${}_{\Lambda}^{11}\text{B}$, and thus the even-parity spin-spin and spin-orbit interactions are important to reproduce the energy spacing. Furthermore, one of the observed excited states at 1.48 MeV in ${}_{\Lambda}^{11}\text{B}$ is close to the calculated $(1/2^+, 3/2^+)$ doublet. In ${}_{\Lambda}^{12}\text{C}$, the present calculation nicely reproduces the ground-state doublet $(1_1^-, 2_1^-)$. In addition, the excitation energy of the 1_2^- states at 3.07 MeV is also close to the observed value (2.83 MeV).

In the several hypernuclei, the excitation energies of the doublets are higher than those of the observed states, which is mainly due to the deviation of the core excitation energies from the experiments. For example, in the 1_3^- state of ${}_{\Lambda}^{12}\text{C}$, the calculated excitation energy ($E_x({}^{12}\text{C}; 1_3^-) = 8.01$ MeV) is higher by about 2 MeV than the observed value. Note that the excitation energy of the core state $3/2_2^-$ is overestimated by about 1.8

MeV. By subtracting the energy shift of 1.8 MeV from the excitation energy, the $E_x({}^{12}\text{C}; 1_3^-)$ becomes much close to the observed value (6.05 MeV). The same thing occurs in ${}_{\Lambda}^{16}\text{O}$: the excited $(1_2^-, 2_1^-)$ doublet is rather high in excitation energy, whereas the splitting energy (0.22 MeV) is consistent with the observation. This is mainly due to the overestimation of the excitation energy of the core state $3/2_2^-$ in ${}^{15}\text{O}$, related to the description of the single-particle orbits as mentioned in Sec. IV B. Thus, in these cases, the discrepancy of the excitation energies is attributed to those of the core states. Concerning this fact, in ${}_{\Lambda}^9\text{Li}$, the excitation energy of the $(5/2^+, 7/2^+)$ doublet would be higher by about 0.7 MeV, because the core state 3^+ locates lower than the observed state by 0.71 MeV in ${}^8\text{Li}$.

Let us discuss the excited states of ${}_{\Lambda}^{15}\text{N}$. In ${}_{\Lambda}^{15}\text{N}$, the splitting energy (0.47 MeV) of the $(1/2_2^+, 3/2_2^+)$ doublet is almost the same as the energy spacing (0.48 MeV) of the observed excited states at 4.23 MeV and 4.71 MeV. Therefore these observed states are considered to be $(1/2_2^+, 3/2_2^+)$ doublet. However, the excitation energies are higher by about 0.7 MeV than those of the observed states. Since the deviation of the core state 1_2^+ state in ${}^{14}\text{N}$ from the experiment is only about 0.2 MeV in excitation energy, it is considered that the present calculation slightly overestimates the energy shift by a Λ particle. In Fig. 4, we see shifts of the excitation energy in the other hypernuclei, which are discussed in the next Section.

We give comments on the tensor-force contributions as well as ΛN - ΣN coupling effects in Λ hypernuclei. It is revealed that the tensor components affect splitting energies of spin-doublets of Λ hypernuclei [64–66]. It is also pointed out that the ΛN - ΣN coupling contributes to excitation energies [67–69]. Recently, the ΛN interactions derived from chiral effective field theory have been developed and are used in several hypernuclear structure calculations such as the no-core shell model calculations [70, 71]. For example, in Ref. [70], the competition between the ΛN - ΣN coupling and YNN three-body force is also investigated in p -shell Λ hypernuclei. The ΛN - ΣN coupling affects not only the excitation energies but the bound-state formation of hypernuclei. In Ref. [72], it is showed that the tensor components of the ΛN - ΣN coupling plays an essential role to make light hypernuclei bound.

In the ESC interaction model, the important roles are played by the ΛN - ΣN coupling interactions composed of central and tensor terms. In the G -matrix approach, high-momentum components of these interactions are renormalized into the ΛN - ΛN central interactions. The residual ΛN - ΛN and ΛN - ΣN interactions also composed of central and tensor terms are not taken into account in this work, considering that these low-momentum tensor interactions are usually of minor contributions for the spectra of Λ hypernuclei. Anyway, it is our future subject to take into account ΛN - ΣN and tensor couplings explicitly in our AMD treatments.

Here, let us reveal the importance of the renormalized parts, which is implicit in our results: We have tried to derive the limited YNG interaction from the ESC+MBE model by switching off all tensor forces in ΛN - ΛN and ΛN - ΣN channels, and applied it to perform calculations for ${}^4_\Lambda\text{H}$, ${}^7_\Lambda\text{Li}$, and ${}^9_\Lambda\text{Be}$. Then, the differences from the above results demonstrate the tensor-force contributions. First of all, these hypernuclei are found to be unbound when the tensor-force contributions are switched off in deriving the limited YNG interaction. Here, the dominant contribution to the tensor-force renormalization comes from the ΛN - ΣN SD -coupling tensor term. This shows an essential role of the ΛN - ΣN tensor coupling for bound-state formation of Λ hypernuclei. It is also found that switching off the tensor contributions changes the spin-spin splitting in the excitation spectra dramatically, while the spin-orbit splittings are not affected so significantly. In ${}^4_\Lambda\text{H}$, the excitation energy of the 1^+ state from the ground 0^+ state, $E_x({}^4_\Lambda\text{H}; 1^+)$, is shifted up and becomes $E_x({}^4_\Lambda\text{H}; 1^+) = 2.05$ MeV with the tensor contribution being switched off, which is compared to the experimental value $E_x^{\text{exp}}({}^4_\Lambda\text{H}; 1^+) = 1.09$ MeV. This is mainly due to the reduction of the 3E attraction dominated in the 1^+ state by switching off the tensor components, whereas the singlet-even (1E) force with no tensor component is important in the ground state 0^+ . In ${}^7_\Lambda\text{Li}$, the excitation energy of the $3/2^+$ state becomes $E_x({}^7_\Lambda\text{Li}; 3/2^+) = 1.53$ MeV, which is much higher than the experimental value $E_x^{\text{exp}}({}^7_\Lambda\text{Li}; 3/2^+) = 0.69$ MeV. Thus, it is demonstrated that the bare tensor forces in the ESC model affect significantly hypernuclear bound-state formations and spin-doublet splittings. We emphasize that this mechanism of taking account of tensor-force effect is sufficiently represented as the effective central attraction under the G -matrix approximation.

Next, we discuss the charge dependence of the ΛN interaction. In the $A = 4$ hypernuclei, the B_Λ values of the ground states are known to be different: $B_\Lambda = 2.04 \pm 0.04$ MeV in ${}^4_\Lambda\text{H}$ and $B_\Lambda = 2.39 \pm 0.03$ MeV in ${}^4_\Lambda\text{He}$ [63]. Recently, in ${}^4_\Lambda\text{He}$, the excitation energy of the 1^+ is precisely measured by the γ -ray spectroscopy experiment [73]. The reported value is $E_x({}^4_\Lambda\text{He}; 1^+) = 1.406 \pm 0.004$ MeV, which is much larger than $E_x({}^4_\Lambda\text{H}; 1^+) = 1.09 \pm 0.02$ MeV. These facts indicate that the ΛN interaction has the charge dependence. Since the ${}^4_\Lambda\text{H}$ and ${}^4_\Lambda\text{He}$ are the mirror hypernuclei, this fact is referred to the charge symmetry breaking (CSB). One can expect that the CSB affects the spin-doublet splitting as well as the Λ binding energies (B_Λ). In this study, we evaluate the CSB effects using the phenomenological CSB force, which is given by the same functional form as in Ref.[74], namely,

$$v^{\text{CSB}}(r) = -\frac{\tau_z}{2} \left[\frac{1 + P_x}{2} (v_0^{\text{E,CSB}} + \vec{\sigma} \cdot \vec{\sigma} v_\sigma^{\text{E,CSB}}) e^{-r^2} + \frac{1 - P_x}{2} (v_0^{\text{O,CSB}} + \vec{\sigma} \cdot \vec{\sigma} v_\sigma^{\text{O,CSB}}) e^{-r^2} \right].$$

As shown in Fig. 5, we determine the parameters of even-parity part $v_0^{\text{E,CSB}}$ and $v_\sigma^{\text{E,CSB}}$ so as to reproduce the

experimental data of ${}^4_\Lambda\text{H}$ and ${}^4_\Lambda\text{He}$, where the odd-parity parts ($v_0^{\text{O,CSB}}$ and $v_\sigma^{\text{O,CSB}}$) are zero. The resulting values are $v_0^{\text{E,CSB}} = 10.0$ MeV and $v_\sigma^{\text{E,CSB}} = 1.5$ MeV. We apply this CSB force to several $N \neq Z$ hypernuclei, ${}^9_\Lambda\text{Li}$, ${}^{10}_\Lambda\text{Be}$ and ${}^{10}_\Lambda\text{B}$. It is found that the B_Λ values are reduced by 0.27 MeV and 0.12 MeV in ${}^9_\Lambda\text{Li}$ and ${}^{10}_\Lambda\text{Be}$, respectively, while B_Λ is increased by 0.12 MeV in ${}^{10}_\Lambda\text{B}$, depending on the balance of the proton and neutron numbers. On the other hand, the changes of the excitation energies are about 40 keV at maximum. Therefore the CSB indicated by the ${}^4_\Lambda\text{H}$ and ${}^4_\Lambda\text{He}$ data does not affect the spin-doublet splitting of the p -shell hypernuclei significantly.

Finally, we also give a comment on the excitation spectra calculated with the NSC97f force that is characterized by the strong repulsion of the odd-state interaction, whereas that is weakly repulsive in the ESC14 model. It is noted that the central and tensor forces of the ΛN - ΣN coupling are renormalized in NSC97f by the G -matrix calculation. It was pointed out that the central force of NSC97f gives the better agreement of the spin doublet splitting energies in several p -shell hypernuclei [26], while its spin-orbit force gives larger splitting energy. Using the central force of NSC97f, the splitting energies of the ground-state doublets are calculated as 1.11 MeV and 0.60 MeV in ${}^4_\Lambda\text{H}$ (0^+ and 1^+) and ${}^7_\Lambda\text{Li}$ ($1/2^+$ and $3/2^+$), respectively, which are almost consistent with the observed values. However, it is necessary to tune the spin-orbit force. In ${}^9_\Lambda\text{Be}$, the splitting energy of the ($3/2^+$, $5/2^+$) doublet is 500 keV using the original parameter set of the spin-orbit force of NSC97f, which is much larger than the observed value (40 keV) and that with the original parameter set of ESC14+MBE. Therefore, we introduce a factor α_{ALS} multiplied to the ALS force to control the cancellation between the SLS and ALS forces, in the same manner as in Sec. IV B. It is found that $\alpha_{\text{ALS}} = 5.5$ gives a reasonable value of the splitting energy (50 keV) in ${}^9_\Lambda\text{Be}$, which is much larger than that determined with ESC14+MBE ($\alpha_{\text{ALS}} = 1.9$). This corresponds to the larger splitting energy with the original spin-orbit force of NSC97f. Using both the central and above spin-orbit forces, it is found that the NSC97f interaction gives similar results of the excitation spectra of the p -shell hypernuclei to those using the ESC14+MBE.

E. Energy shifts by the addition of a Λ particle

In this Section, we discuss the change of the excitation energies in the hypernuclei in comparison with the core nuclei. In general, energy shifts are caused by spin-dependent nature of the ΛN interaction [67, 68]. For example, the ΛN spin-orbit interaction depending on the nuclear spin plays an essential role for energy shifts in hypernuclei. Recently, it is also discussed that the difference of nuclear radii in core states affects the energy shifts of the corresponding states in the hypernuclei [23]. It should be noted that both of these effects are included in our results.

TABLE III: Calculated total (E), excitation (E_x), and Λ binding (B_Λ) energies for each state in the hypernuclei in unit of MeV. Experimental values of the Λ binding energy B_Λ^{exp} [MeV] in the ground states are also shown. In ${}^{16}_\Lambda\text{O}$, the B_Λ^{exp} value with † is shifted deeper by 0.54 MeV from that measured by the (π^+, K^+) reaction experiemnt [60], concerning the systematic difference of B_Λ^{exp} between the emulsion and (π^+, K^+) experiments reported in Ref. [55]. The Fermi momentum k_F [fm^{-1}] used in this calculation and nuclear root-mean-square radius r_{rms} [fm] are also shown. In comparison, E , E_x , and r_{rms} are also listed for the corresponding core states.

Hypernuclei	k_F	J^π	E	E_x	r_{rms}	B_Λ	B_Λ^{exp}	Core nuclei	J^π	E	E_x	r_{rms}
${}^7_\Lambda\text{Li}$	1.05	1/2 ⁺	-45.69	0.00	2.28	5.66	5.58 ± 0.03 [61]	${}^6\text{Li}$	1 ⁺	-40.03	0.00	2.34
		3/2 ⁺	-45.02	0.67	2.28	4.99						
		5/2 ⁺	-43.84	1.85	2.19	6.02			3 ⁺	-37.82	2.21	2.24
		7/2 ⁺	-43.35	2.33	2.19	5.53						
${}^9_\Lambda\text{Li}$	1.02	3/2 ⁺	-54.04	0.00	2.38	9.20	8.50 ± 0.12 [62]	${}^8\text{Li}$	2 ⁺	-44.84	0.00	2.43
		5/2 ⁺	-53.71	0.33	2.37	8.87						
		5/2 ⁺	-53.00	1.04	2.31	9.71			3 ⁺	-43.29	1.55	2.36
		7/2 ⁺	-52.56	1.47	2.31	9.27						
${}^9_\Lambda\text{Be}$	1.12	1/2 ⁺	-61.67	0.00	2.39	6.81	6.71 ± 0.04 [63]	${}^8\text{Be}$	0 ⁺	-54.86	0.00	2.48
		5/2 ⁺	-58.85	2.82	2.39	6.89			2 ⁺	-51.91	2.95	2.49
		3/2 ⁺	-58.80	2.87	2.39	6.94						
${}^{10}_\Lambda\text{Be}$	1.10	1 ⁻	-62.76	0.00	2.31	8.68	8.55 ± 0.18 [55]	${}^9\text{Be}$	3/2 ⁻	-54.07	0.00	2.40
		2 ⁻	-62.60	0.16	2.31	8.53						
		2 ⁻	-60.16	2.60	2.30	8.57			5/2 ⁻	-51.59	2.49	2.40
		3 ⁻	-60.00	2.76	2.30	8.41						
		3 ⁻	-56.18	2.58	2.26	8.94			7/2 ⁻	-47.24	6.83	2.37
		4 ⁻	-56.16	2.60	2.26	8.92						
${}^{10}_\Lambda\text{B}$	1.09	1 ⁻	-60.76	0.00	2.35	8.87	8.89 ± 0.12 [63]	${}^9\text{B}$	3/2 ⁻	-51.89	0.00	2.46
		2 ⁻	-60.58	0.18	2.35	8.69						
		2 ⁻	-58.15	2.61	2.34	8.72			5/2 ⁻	-49.43	2.46	2.46
		3 ⁻	-58.05	2.71	2.34	8.62						
${}^{11}_\Lambda\text{B}$	1.05	5/2 ⁺	-82.33	0.00	2.45	11.18	10.24 ± 0.05 [63]	${}^{10}\text{B}$	3 ⁺	-71.15	0.00	2.49
		7/2 ⁺	-81.95	0.38	2.44	10.80						
		1/2 ⁺	-80.80	1.53	2.48	10.24			1 ⁺	-70.56	0.59	2.52
		3/2 ⁺	-80.77	1.55	2.46	10.21						
		1/2 ⁺	-79.14	3.19	2.52	10.43			1 ⁺	-68.71	2.44	2.54
		3/2 ⁺	-78.88	3.44	2.52	10.17						
${}^{12}_\Lambda\text{C}$	1.08	1 ⁻	-90.22	0.00	2.45	12.28	10.76 ± 0.19 [62]	${}^{11}\text{C}$	3/2 ⁻	-77.94	0.00	2.49
		2 ⁻	-90.09	0.13	2.45	12.15						
		1 ⁻	-87.15	3.07	2.52	11.26			1/2 ⁻	-75.89	2.05	2.55
		0 ⁻	-86.93	3.29	2.52	11.04						
		2 ⁻	-85.70	4.52	2.49	11.55			5/2 ⁻	-74.15	3.79	2.52
		3 ⁻	-85.51	4.71	2.49	11.36						
		2 ⁻	-82.39	7.83	2.54	11.02			3/2 ⁻	-71.37	6.57	2.54
		1 ⁻	-82.21	8.01	2.54	10.84						
${}^{13}_\Lambda\text{C}$	1.10	1/2 ⁺	-105.74	0.00	2.47	12.29	11.69 ± 0.19 [61]	${}^{12}\text{C}$	0 ⁺	-92.82	0.00	2.53
		5/2 ⁺	-100.98	4.76	2.52	12.25			2 ⁺	-88.73	4.09	2.56
		3/2 ⁺	-100.91	4.83	2.52	12.18						
${}^{15}_\Lambda\text{N}$	1.13	3/2 ⁺	-125.15	0.00	2.54	13.70	13.59 ± 0.15 [63]	${}^{14}\text{N}$	1 ⁺	-111.45	0.00	2.56
		1/2 ⁺	-124.98	0.16	2.54	13.53						
		3/2 ⁺	-120.23	4.92	2.58	12.94			1 ⁺	-107.29	4.16	2.59
		1/2 ⁺	-120.00	5.15	2.59	12.71						
${}^{16}_\Lambda\text{O}$	1.16	1 ⁻	-127.56	0.00	2.57	13.49	12.96 ± 0.05 †[60]	${}^{15}\text{O}$	1/2 ⁻	-114.07	0.00	2.57
		0 ⁻	-127.38	0.18	2.57	13.31						
		1 ⁻	-116.93	10.63	2.62	12.70			3/2 ⁻	-104.23	9.84	2.62
		2 ⁻	-116.71	10.85	2.62	12.48						

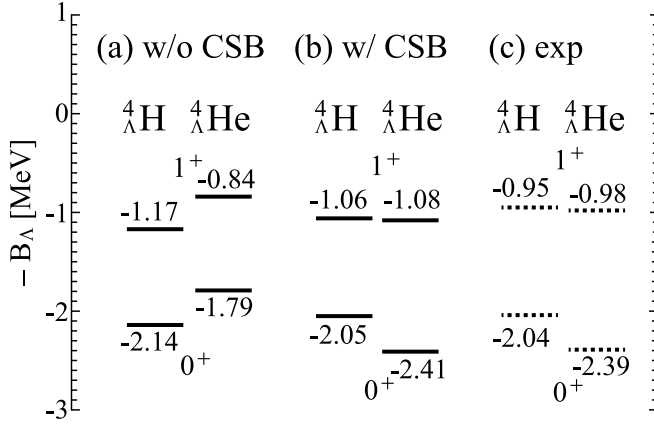


FIG. 5: (a) Calculated energy spectra of ${}^4_{\Lambda}\text{H}$ and ${}^4_{\Lambda}\text{He}$ using ESC+MBE with $k_F = 0.92 \text{ fm}^{-1}$. (b) Same as (a), but with the phenomenological charge symmetry breaking (CSB) force explained in text. (c) Experimental data taken from Refs. [63, 73].

Figure 4 shows that in the most hypernuclei the excitation energies of the excited doublets are shifted from the corresponding core states. For example, in ${}^{11}_{\Lambda}\text{B}$, the $(1/2_1^+, 3/2_1^+)$ and $(1/2_2^+, 3/2_2^+)$ doublets are largely shifted up in the excitation spectra compared to the 1_1^+ and 1_2^+ states in ${}^{10}\text{B}$. In a more rigorous discussion, to remove the splitting energies of the doublets, the difference of the centroid energies between the ground and excited doublets should be compared with the excitation energies in the core nuclei. In ${}^{11}_{\Lambda}\text{B}$, the centroid energy differences between the ground and two excited doublets, $(1/2_1^+, 3/2_1^+)$ and $(1/2_2^+, 3/2_2^+)$, are 1.25 MeV and 3.09 MeV, corresponding to the energy shifts of 0.66 MeV and 0.65 MeV, respectively. The large shift up is also seen in the excited doublets of ${}^{12}_{\Lambda}\text{C}$, ${}^{15}_{\Lambda}\text{N}$ and ${}^{16}_{\Lambda}\text{O}$. On the other hand, in the Li hypernuclei, it is seen that the addition of the Λ particle decreases the excitation energies. For example, in ${}^9_{\Lambda}\text{Li}$, the difference of the centroid energies between the ground and $(5/2^+, 7/2^+)$ doublets is 1.12 MeV, which is smaller than the excitation energy (1.57 MeV) of the 3^+ state in ${}^8\text{Li}$.

It is pointed out that the energy shifts caused by a Λ particle are closely related to the difference of the nuclear radii [23]. In Ref. [23], based on the microscopic α cluster model calculation for p shell Λ hypernuclei, it is shown that the excitation energy shift is correlated with the difference of the nuclear size. This is because the Λ particle in s orbit penetrates into nuclear interior, which probes nuclear density through the ΛN interaction. Increasing the nuclear radius makes the overlap between the Λ particle and nucleons smaller, which results in decreases of the Λ binding energy, whereas the Λ particle is deeply bound in a spatially compact state. The difference of the Λ binding energies depending on the size of each state causes the energy shifts in excitation spectra. Similar phenomena were pointed out in deformed states, where

increasing the nuclear quadrupole deformation makes the Λ binding energy shallower corresponding to the smaller overlap between the Λ and nucleons in deformed states [75, 76].

In the present results, we see the correlation between the energy shifts and nuclear radii. In ${}^{11}_{\Lambda}\text{B}$, ${}^{12}_{\Lambda}\text{C}$, ${}^{15}_{\Lambda}\text{N}$ and ${}^{16}_{\Lambda}\text{O}$, the excited states are shifted up by the addition of a Λ particle, indicating that the Λ binding energy is smaller in the excited states than the ground states. In Tab. III, we see the difference in the nuclear root-mean-square radii (r_{rms}) and in the Λ binding energies B_{Λ} between the ground and excited states. Here, the B_{Λ} is defined not only for the ground state but also excited states as the energy gain from the corresponding core state. For example, in ${}^{11}_{\Lambda}\text{B}$, the B_{Λ} values are about 10.2 MeV in the excited doublets $(1/2_1^+, 3/2_1^+)$ and $(1/2_2^+, 3/2_2^+)$, whereas $B_{\Lambda} = 11.18 \text{ MeV}$ and 10.80 MeV in the ground state doublet, which causes the energy shift up of the excited doublets. It is found that the difference of B_{Λ} corresponding to that of the nuclear radii. In the core nucleus of ${}^{11}\text{B}$, ${}^{10}\text{B}$, the calculated values of r_{rms} are 2.52 fm and 2.54 fm in the 1_1^+ and 1_2^+ states, respectively, whereas $r_{\text{rms}} = 2.49 \text{ fm}$ in the ground state 3^+ . In the corresponding states in ${}^{11}_{\Lambda}\text{B}$, the nuclear radii are larger in the excited doublets $(1/2_1^+, 3/2_1^+)$ and $(1/2_2^+, 3/2_2^+)$ than the ground-state doublet after the shrinkage of the system with the Λ particle. On the other hand, in ${}^7_{\Lambda}\text{Li}$ and ${}^9_{\Lambda}\text{Li}$, where the excited doublets are shifted down in the excitation spectra, the nuclear radii of the excited states are smaller than the ground state. For example, in ${}^7_{\Lambda}\text{Li}$, the r_{rms} is 2.19 fm in the excited doublet $(5/2^+, 7/2^+)$, which is smaller than those in the ground state doublet ($r_{\text{rms}} = 2.28 \text{ fm}$). The trend of the energy shift down or up in ${}^7_{\Lambda}\text{Li}$, ${}^{11}_{\Lambda}\text{B}$, ${}^{12}_{\Lambda}\text{C}$, and ${}^{15}_{\Lambda}\text{N}$ is consistent with the results in Ref. [23].

V. SUMMARY

We investigate the spin-spin and spin-orbit splittings of the p -shell Λ hypernuclei within the framework of HyperAMD with the ΛN G -matrix interaction ESC14+MBE. In Ref. [25], it is shown that the mass dependence of the B_{Λ} values are nicely reproduced by describing the nuclear core structure within the framework of the HyperAMD with the latest version of the YNG interaction, ESC14+MBE. At the same time, however, this preceding analysis showed the discrepancy in energy level order of ground-state spin doublets. This fact tells us that there is a room to correct the spin-dependent parts of ESC14+MBE.

In this paper, we make an adjustment of the ΛN spin-spin and spin-orbit interactions derived from ESC14+MBE. Since the central force of the ESC14+MBE has a three range Gaussian form, we add correction terms $\Delta V^E \exp[-(r/\beta_2)^2]$ and $\Delta V^O \exp[-(r/\beta_2)^2]$ to the even and odd state interactions of the ΛN spin-spin force, respectively. By the anal-

ysis and comparison with the observed data in ${}^4_\Lambda\text{H}$ and ${}^7_\Lambda\text{Li}$, we determine the strength of the correction terms as $\Delta V^E = 1.2$ MeV and $\Delta V^O = 30.0$ MeV. The spin-orbit force of the ESC14+MBE is tuned by multiplying a correction factor α_{ALS} to the ALS force to control the cancellation between the SLS and ALS forces. In ${}^9_\Lambda\text{Be}$, it is found that the splitting energy of the $(3/2^+, 5/2^+)$ doublet decreases as the α_{ALS} increases, and thus we determine $\alpha_{ALS} = 1.9$ to reproduce the experimental value of energy spacing.

Using the tuned version of the ESC14+MBE, we have applied the HyperAMD to ten p -shell Λ hypernuclei, namely ${}^7_\Lambda\text{Li}$, ${}^9_\Lambda\text{Li}$, ${}^9_\Lambda\text{Be}$, ${}^{10}_\Lambda\text{Be}$, ${}^{10}_\Lambda\text{B}$, ${}^{11}_\Lambda\text{B}$, ${}^{12}_\Lambda\text{C}$, ${}^{13}_\Lambda\text{C}$, ${}^{15}_\Lambda\text{N}$, and ${}^{16}_\Lambda\text{O}$. The present calculation reproduces not only the ground-state spin of these hypernuclei systematically but also the energy spacing of the ground and excited doublets satisfactorily.

In most cases, it is remarkable that the excitation energies of the excited states in the hypernuclei are different from those of the corresponding core states, *i.e.* the energy shifts occur by the addition of a Λ particle. It is

found that the excitation energies are shifted up in the excited states with larger radii than the ground state in the hypernuclei, whereas the spatially compact excited states are lowered in excitation energy by adding a Λ particle. This is mainly due to the difference of the Λ binding energies between the ground and excited states, which decrease as the nuclear radius increases.

In conclusion, we have obtained successful description of p -shell hypernuclear structures by making additional tuning of both even- and odd-state spin-dependent components of G -matrix derived from the fundamental baryon-baryon interaction ESC14+MBE. Thus, we have proposed a new practical set of the YNG parameters of G -matrix interactions to be applied further to a wide mass region. Using this interaction together with the hypernuclear structure models including HyperAMD, it will be possible to predict various phenomena caused by a Λ particle such as nuclear structure changes in hypernuclei, which can be compared with existing and/or future experiments quantitatively.

-
- [1] O. Hashimoto and H. Tamura, Prog. Part. and Nucl. Phys. **57**, 564 (2006).
 - [2] P. M. M. Maessen, T. A. Rijken, and J. J. de Swart, Phys. Rev. C **40**, 2226 (1989).
 - [3] Th. A. Rijken, V. G. J. Stoks, and Y. Yamamoto, Phys. Rev. C **59**, 21 (1999).
 - [4] Th. A. Rijken and Y. Yamamoto, Phys. Rev. C **73**, 044008 (2006).
 - [5] Th. A. Rijken, M. M. Nagels, and Y. Yamamoto, Prog. Theor. Phys. Suppl. **185**, 14 (2010).
 - [6] B. Holzenkamp, K. Holinde, and J. Speth, Nucl. Phys. A **500**, 485 (1989).
 - [7] A. Reuber, K. Holinde, and J. Speth, Nucl. Phys. A **570**, 543 (1994).
 - [8] Y. Fujiwara, Y. Suzuki, and C. Nakamoto, Prog. Part. Nucl. Phys. **58**, 439 (2007).
 - [9] T. Motoba, H. Bando, and K. Ikeda, Prog. Theor. Phys. **70**, 189 (1983).
 - [10] T. Motoba, H. Bando, K. Ikeda, and T. Yamada, Prog. Theor. Phys. Suppl. **81**, 42 (1985).
 - [11] E. Hiyama, M. Kamimura, K. Miyazaki, and T. Motoba, Phys. Rev. C **59**, 2351 (1999).
 - [12] K. Tanida, H. Tamura, D. Abe, H. Akikawa, K. Araki, H. Bhang, T. Endo, Y. Fujii, T. Fukuda, O. Hashimoto et al., Phys. Rev. Lett. **86**, 1982 (2001).
 - [13] X.-R. Zhou, H.-J. Schulze, H. Sagawa, C.-X. Wu, and E.-G. Zhao, Phys. Rev. C **76**, 034312 (2007).
 - [14] M. T. Win and K. Hagino, Phys. Rev. C **78**, 054311 (2008).
 - [15] H.-J. Schulze, M. T. Win, K. Hagino, and H. Sagawa, Prog. Theor. Phys. **123**, 569 (2010).
 - [16] M. Isaka, M. Kimura, A. Dote, and A. Ohnishi, Phys. Rev. C **83**, 044323 (2011).
 - [17] B.-N. Lu, E.-G. Zhao, and S.-G. Zhou, Phys. Rev. C **84**, 014328 (2011).
 - [18] H. Mei, K. Hagino, J. M. Yao, and T. Motoba, Phys. Rev. C **90**, 064302 (2014).
 - [19] W. X. Xue, J. M. Yao, K. Hagino, Z. P. Li, H. Mei, and Y. Tanimura, Phys. Rev. C **91**, 024327 (2015).
 - [20] J.-W. Cui, X.-R. Zhou, and H.-J. Schulze, Phys. Rev. C **91**, 054306 (2015).
 - [21] E. Hiyama, M. Kamimura, T. Motoba, T. Yamada, and Y. Yamamoto, Phys. Rev. Lett. **85**, 270 (2000).
 - [22] M. Isaka, M. Kimura, A. Dote, and A. Ohnishi, Phys. Rev. C **83**, 054304 (2011).
 - [23] Y. Kanada-En'yo, Phys. Rev. C **97**, 024330 (2018).
 - [24] M. Isaka, Y. Yamamoto and Th. A. Rijken, Phys. Rev. C **94**, 044310 (2016).
 - [25] M. Isaka, Y. Yamamoto and Th. A. Rijken, Phys. Rev. C **95**, 044308 (2017).
 - [26] Y. Yamamoto, T. Motoba, Th. A. Rijken, Prog. Theor. Phys. Suppl. **No.185**, 72 (2010).
 - [27] T. Motoba, D.J. Millener, D.E. Lansky, and Y. Yamamoto, Nucl. Phys. A **804**, 99 (2008).
 - [28] E. Hiyama, M. Kamimura, Y. Yamamoto and T. Motoba, Phys. Rev. Lett. **104**, 212502 (2010).
 - [29] J. Decharge and D. Gogny, Phys. Rev. C **21**, 1568 (1980).
 - [30] J. F. Berger, M. Girod, and D. Gogny, Comput. Phys. Commun. **63**, 365 (1991).
 - [31] A. Volkov, Nucl. Phys. **74**, 33 (1965).
 - [32] J. P. Elliot, Proc. Roy. Soc. London, **A245**, 128, 562 (1958).
 - [33] M. Harvey, in *Advances in Nuclear Physics*, Vol.1 (eds. M. Baranger and E. Vogt), Plenum Press N. Y. (1968), and references therein.
 - [34] Y. Miura et al., Nuclear Phys. A **754**, 75c(2005)
 - [35] K. Hosomi, et al., Prog. Theor. Exp. Phys. **2015**, 081D01(2015)
 - [36] L. Tang et al., Phys. Rev. C **90**, 034320 (2014).
 - [37] T. Motoba, JPS Conf. Proc. **17**, 011003 (2017).
 - [38] Y. Kanada-En'yo, Phys. Rev. Lett. **81**, 5291 (1998)
 - [39] N. Itagaki, S. Aoyama, S. Okabe, and K. Ikeda, Phys. Rev. C **70**, 054307(2004).
 - [40] T. Neff and H. Feldmeier, Nucl. Phys. A **738**, 357 (2004).

- [41] Y. Kanada-En'yo, Prog. Theor. Phys. **117**, 655 (2007)
- [42] Y. Kanada-En'yo, M. Kimura, and A. Ono, Prog. Theor. Exp. Phys. **2012**, 01A202 (2012).
- [43] T. Suhara and Y. Kanada-En'yo, Phys. Rev. C **91**, 024315 (2015)
- [44] N. Yamaguchi, T. Kasahara, S. Nagata, and Y. Akaishi, Prog. Theor. Phys.**62**, 1018 (1979).
- [45] D.R. Tilley, et al, Nucl. Phys. A**708**, 3(2002)
- [46] J.H. Kelley, et al, Nucl. Phys. A**880**, 88(2012)
- [47] J.H. Kelley, et al, Nucl. Phys. A**968**, 71(2017)
- [48] F. Ajzenberg-selove, Nucl. Phys. A**523**, 1(1991)
- [49] D.R. Tilley, et al, Nucl. Phys. A**745**, 155(2004)
- [50] A. Bamberger et al., Phys. Lett. B**36**, 412(1971) 412; Nuclear Phys. B**60**, 1(1973)
- [51] M. Bedjidian et al., Phys. Lett. B**62**, 467(1976)
- [52] M. May et al., Phys. Rev. Lett. **51**, 2085(1983)
- [53] H. Tamura et al., Phys. Rev. Lett. **84**, 5963(2000)
- [54] H. Akikawa et al., Phys. Rev. Lett. **88**, 082501(2002)
- [55] T. Gogami, et al., Phys. RevC**93**, 034314(2016)
- [56] H. Tamura, Nuclear Phys. A**754**, 58c(2005) 58c
- [57] R.E. Chrien et al., Phys. Rev. C**41**, 1062(1990)
- [58] H. Kohri, et al., Phys. Rev.C**65**, 034607(2002)
- [59] M. Ukai et al., Phys. Rev. Lett. **93**, 232501(2004)
- [60] S. Ajimura et al., Nucl. Phys. A**639**, 93c (1998)
- [61] D. H. Davis, Nucl. Phys. A**547**, 369 (1992)
- [62] D. H. Davis, Nucl. Phys. A**754**, 3 (2005)
- [63] M. Jurić et al., Nucl. Phys. B **52**, 1 (1973)
- [64] A. Gal, J. M. Soper, and R. H. Dalitz, Ann. Phys. (N.Y.) **63**, 53 (1971)
- [65] Dalitz, R. H., and A. Gal, Ann. Phys. (N.Y.) **116**, 167 (1978).
- [66] D. J. Millener et al., Phys. Rev. C **31**, 499 (1985).
- [67] D.J. Millener, Nucl. Phys. A **754**, 48c (2005).
- [68] D.J. Millener, Nucl. Phys. A **804**, 84 (2008).
- [69] A. Gal, E.V. Hungerford, D.J. Millener, Rev. Mod. Phys. **88**, 035004 (2016).
- [70] Roland Wirth and Robert Roth, Phys. Rev. Lett. **117**, 182501 (2016).
- [71] Roland Wirth and Robert Roth, Phys. Lett. B **779**, 336 (2018).
- [72] H. Nemura, Y. Akaishi, and Y. Suzuki, Phys. Rev. Lett. **89**, 142504(2002).
- [73] T.O. Yamamoto, et al, Phys. Rev. Lett. **115**, 222501 (2015)
- [74] E. Hiyama, Nucl. Phys. A **835**, 215(2010)
- [75] M. Isaka, K. Fukukawa, M. Kimura, E. Hiyama, H. Sagawa, and Y. Yamamoto, Phys. Rev. C**89**, 024310 (2014)
- [76] M. Isaka and M. Kimura, Phys. Rev. C**92**, 044326 (2015)